

STUDIES OF PARATUBERCULOSIS OF RED DEER

VOLUME 2

Tables and Figures



TABLES

Table 1.0 Wild ruminants affected with paratuberculosis

Species	Environment	Reference
Red deer (<u>Cervus elaphus</u>)	park and farmed	McFadyean (1907), Bourgeois (1940), Vance (1961), Gumbrell (1987), Jørgensen & Jørgensen (1987), McKelvey (1987)
Sika deer (<u>Pseudaxis sika</u> & <u>Cervus nippon</u>)	park	Bourgeois (1944), Temple, Muscoplat, Thoen, Himes & Johnson (1979)
Reindeer (<u>Rangifer tarandus</u>)	free-living	Katic (1961)
Roe deer (<u>Capreolus capreolus</u>)	free-living	Hillermark (1966)
Moose (<u>Alces alces</u>)	captive	Soltys, Address & Fletch (1967)
White-tailed deer (<u>Odocoileus virginianus</u>)	farmed	Libke & Walton (1975), Chioldini & Van Kruiningen (1983a)
Fallow deer (<u>Dama dama</u>)	park	Riemann, Zaman, Ruppner, Aalund, Jørgensen, Worsaae & Behymer (1979), Temple <u>et al.</u> (1979)
Axis deer (<u>Axis axis</u>)	park	Riemann <u>et al.</u> (1979), Commichau (1982)
Tule elk (<u>Cervus elaphus nannodes</u>)	park	Jessup, Abbas, Behymer & Gogan (1981)
Pere David's deer (<u>Elaphurus davidianus</u>)	park/farmed	Buxton (1987)
Gnu (<u>Connochaetes albobatus</u>)	captive	Katic (1961)
Stonebuck (<u>Capra aegagrus ibex</u> L.)	park	Hillermark (1966)
African buffalo (<u>Syncerus caffer</u>)	captive	Katic (1961)
Yak (<u>Bos grunniens</u>)	park	Almejew (1958)
Aoudad (<u>Ammotragus lervia</u>)	park	Boever & Peters (1974)
Mouflon (<u>Ovis musimon</u>)	park	Boever & Peters (1974)
Bighorn sheep (<u>Ovis canadensis</u>)	free-living	Williams & Spraker (1979)
Rocky Mountain goat (<u>Oreamnos americanus</u>)	free-living	Williams & Spraker (1979)

Table 3.1. Summarized results of mesenteric lymph node histopathology and culture for M. paratuberculosis in normal red deer originating from an affected herd (A)

Year	No. examined	Histopathology:		Culture: No. (%) positive
		No. (%) positive with 1. lesions	2. organisms	
1st	167 (NV)	64 (38.3)	36 (21.6)	NT
2nd	201 (V)	31 (15.4)	9 (4.5)	29 (14.4)
	15 (NV)	4 (26.7)	4 (26.7)	5 (33.3)
3rd	47 (V)	13 (27.7)	2 (4.3)	15 (31.9)

NT = not tested
(V) = vaccinated
(NV) = non-vaccinated

Table 3.2. The relationship of the results of histopathology and culture for the 2nd and 3rd years

Year	No. examined	No. (%) pos. (combined results)	No. (%) histo. & cult. pos.	No. (%) histo. pos. but cult. neg.	No. (%) cult. pos. but histo. neg.
2nd	201 (V)	41 (20.4)	19 (9.4)	12 (6.0)	10 (5.0)
	15 (NV)	5 (33.3)	4 (26.7)	0	1 (6.7)
3rd	47 (V)	22 (46.8)	6 (12.8)	7 (14.9)	9 (19.1)

V = vaccinated
 NV = non-vaccinated

Table 3.3. Summarized results of faecal examination and serology for paratuberculosis in clinical cases of naturally infected red deer

Ear tag No.	Source	Faecal examination	Serology
Z21	Farm A	+	+
D25	Farm A	+	+
113	Farm B	-	-
114	Farm B	-	-
69	Farm B	+	-
70	Farm B	+	-

Table 3.4. Distribution of gross pathological lesions in adult red deer hinds naturally infected with M. paratuberculosis

Ear tag No.	Intestines		Mesentery & lymphatic channels	Mesenteric lymph nodes
	Serosa	Mucosa		
Z21	-	-	-	+
D25	+	+	+	+
26	-	NS	-	-
113	-	NS	-	-
114	-	-	-	-
69	+	+	+	+
70	+	+	+	+

NS = non-specific lesions

+ = specific lesions

- = no lesions

Table 3.5. Distribution of histopathological lesions in adult red deer hinds naturally infected with M. paratuberculosis

Ear tag No.	Intestines	Mesentery & lymphatic channels	Mesenteric lymph nodes	Other organs
Z21	+	-	+	+
D25	+	+	+	+
26	NS	-	NS	-
113	-	-	NS	-
114	NS	-	NS	-
69	+	+	+	+
70	+	+	+	+

NS = non-specific lesions
 + = specific lesions
 - = no lesions

Table 3.6. Summarized results of culture for M. paratuberculosis of tissues from adult red deer hinds naturally infected with the organism

Ear tag No.	Intestinal mucosa	Mesenteric lymph nodes	Other tissues
Z21	+	+	-
D25	+	+	-
26	-	+	-
113	-	+	-
114	-	+	-
69	+	+	-
70	+	+	-

+ = M. ptbc cultured
 - = not cultured

Table 4.1. Summary of results of oral experimental infection of red deer calves with M. paratuberculosis and M. avium

Group and animal No.	Clinical disease	Faecal ⁺⁺ excretion of organisms	DTH response	Serology	Pathology (week of killing)	Culture of tissues
<u>M. ptb</u> infected						
78	+	+	+	+	+	+
99	-	-	+	-	+	+
107	+	+	-	+	+	+
109	-	-	+	-	+	+
166	+	+	+	+	+	+
<u>M. avium</u> infected						
121	+	+	NT	-	+	+
124	+	+	NT	-	+	+
161	+	+	NT	-	+	+
Control						
122	-	-	+	-	+	+
141	-	-	-	-	-	-
163	-	-	-	-	NT	NT
164	-	-	-	-	NT	NT

NT - not tested
 + = positive
 - = negative
 ++ = determined by microscopic examination and culture of faeces

Table 4.2. Comparative intradermal tuberculin test responses to avian and bovine tuberculin PPDs of red deer calves experimentally infected with M. paratuberculosis

Group and animal No.	72h increase, in mm, of skin fold thickness and diameter of skin swelling (cm) during weeks					
	8		16		36	
	Avian	Bovine	Avian	Bovine	Avian	Bovine
<u>M. ptbc</u> infected						
78	2.0 (3.5)	3.5 (3.0)	1.0 (2.5)	2.0 (NS)	0.0 (1.0)	0.0 (NS)
99	7.0 (3.5)	2.5 (2.0)	1.0 (2.0)	0.0 (NS)	1.0 (2.0)	0.0 (NS)
107	0.0 (NS)	0.0 (NS)		D		
109	8.0 (4.0)	4.5 (2.0)	2.0 (3.0)	1.0 (1.0)	1.0 (1.0)	0.0 (NS)
166	5.0 (2.5)	3.0 (2.5)	1.0 (2.0)	1.0 (NS)		D
Control						
122	3.0 (2.5)	1.0 (NS)	2.0 (1.5)	1.0 (NS)	1.0 (1.0)	0.0 (NS)
141, 163 & 164	0.0 (NS)	0.0 (NS)	0.0 (NS)	0.0 (NS)	0.0 (NS)	0.0 (NS)

NS = no swelling

D = dead

Table 4.3. Distribution of gross pathological lesions in red deer calves experimentally infected with *M. paratuberculosis* and *M. avium*

Group and animal No.	Serosa	Intestines Mucosa	Mesentery	Mesenteric lymph nodes	Other organs
<u>M. ptbc</u> infected					
78	-	+	-	+	-
99	-	-	-	+	-
107	+	+	+	+	NS
109	-	-	-	+	-
166	-	+	-	+	-
<u>M. avium</u> infected					
121	+	+	+	+	NS
124	-	+	-	+	NS
161	+	+	+	+	NS
Control					
122	-	-	-	+	-
141	-	-	-	-	-

NS = non-specific lesions
+ = specific lesions
- = no lesions

Table 4.4. Distribution of histopathological lesions in red deer calves experimentally infected with M. paratuberculosis and M. avium

Group & animal No.	Small intestine		Large intestines		Mesentery	Mesenteric lymph nodes	Other organs
	Ileum	Jejunum	Duodenum	Caecum			
<u>M. ptbc</u> infected							
78	-	DN	-	-	-	+	-
99	-	-	-	-	-	+	-
107	+	+	+	+	+	+	+
109	-	-	-	-	-	+	-
166	+	-	-	-	-	+	-
<u>M. avium</u> infected							
121	+	+	+	+	+	+	+
124	+	-	-	+	-	+	+
161	+	+	+	+	+	+	+
Control							
122	-	-	-	-	-	+	-
141	-	-	-	-	-	-	-

DN = discrete nodule
+ = specific lesions
- = no lesions

Table 4.5. Summary of results of oral experimental infection of lambs with M. paratuberculosis and M. avium

Group and animal No.	Clinical disease	Faecal excretion of organisms ^{††}	DTH response during weeks 6	DTH response during weeks 14	Serology	Pathology	Culture of tissues
<u>M. ptbce</u> infected							
1779	-	+	-	+	-	+	-
1787	-	-	-	+	-	+	+
1788	-	+	-	+	-	+	-
1789	-	-	-	+	-	+	-
1790	-	+	-	+	-	+	-
1793	-	+	-	+	-	+	-
<u>M. avium</u> infected							
1770	-	+	+	+	-	+	-
1771	-	+	+	+	-	+	-
1775	-	+	+	+	-	+	-
1776	-	-	+	+	-	+	-
1791	-	-	+	+	-	+	+
1792	-	+	+	+	-	+	-
Control							
All (3)	-	-	-	-	-	-	-

+ = positive
 - = negative
 †† = determined by microscopic examination of faeces

Table 4.6. Faecal excretion of organisms in lambs experimentally infected with M. paratuberculosis and M. avium as determined by microscopic examination of faecal smears

Group & animal No.	Week of examination			
	9	12	13	14
<u>M. ptbc</u> infected				
1779	+	+	+	-
1787	+	-	-	-
1788	-	+	+	-
1789	-	-	-	-
1790	-	+	+	-
1793	+	+	+	-
<u>M. avium</u> infected				
1770	+	-	-	-
1771	+	-	-	-
1775	+	-	-	-
1776	-	-	-	-
1791	-	-	-	-
1792	+	-	-	-

+ = AFB detected

- = not detected

Table 4.7. Intradermal comparative tuberculin test responses to avian and bovine tuberculin PPDs of lambs experimentally infected with M. paratuberculosis and M. avium

Group & animal No.	72h increase, in mm, of skin fold thickness during weeks			
	6		14	
	Avian	Bovine	Avian	Bovine
<u>M. ptbc</u> infected				
1779	2.1	0.7	18.4	8.2
1787	1.4	0.7	12.7	5.0
1788	1.3	2.4	15.2	8.9
1789	0.0	0.0	19.1	9.5
1790	0.3	1.6	19.1	6.6
1793	0.3	0.9	17.8	10.2
Median	(0.8)	(0.8)	(18.1)	(8.6)
<u>M. avium</u> infected				
1770	9.2	5.8	17.1	8.8
1771	9.0	9.4	12.4	8.2
1775	16.1	8.6	13.1	6.9
1776	11.1	4.3	12.4	9.2
1791	7.5	3.3	15.1	6.5
1792	12.4	4.6	12.1	9.7
Median	(10.2)	(5.2)	(12.8)	(8.5)

Table 4.8. Distribution of gross pathological lesions in lambs experimentally infected with M. paratuberculosis and M. avium

Group & animal No.	Small intestine		Large intestine	Mesenteric lymph nodes
	ICV & Ileum	Jejunum		
<u>M. ptbc</u> infected				
1779	+	DNs	-	+
1787	+	DNs	-	+
1788	+	-	-	+
1789	+	-	-	+
1790	+	DNs	-	+
1793	+	-	-	+
<u>M. avium</u> infected				
1770	+	-	-	+
1771	+	DNs	-	+
1775	-	-	-	+
1776	+	-	-	+
1791	+	-	-	+
1792	+	DNs	-	+

ICV = ileocaecal valve
 DNs = discrete nodules
 + = specific lesions
 - = no lesions

Table 4.9. Distribution of histopathological lesions in lambs experimentally infected with M. paratuberculosis and M. avium

Group and animal No.	Small intestine		Large intestines		Mesenteric lymph nodes	Retropharyngeal lymph nodes
	ICV & Ileum	Jejunum	Caecum	Colon		
<u>M. ptbc</u> infected						
1779	+	+	-	-	+	-
1787	+	+	+	-	+	-
1788	+	-	-	-	+	-
1789	+	-	+	-	+	-
1790	+	+	+	-	+	-
1793	+	-	+	-	+	+
<u>M. avium</u> infected						
1770	+	-	-	-	+	+
1771	+	+	-	-	+	+
1775	NS	-	-	-	+	+
1776	+	-	-	-	+	+
1791	+	-	+	-	+	-
1792	+	+	+	-	+	+

ICV = ileocaecal valve
 NS = non-specific lesions
 + = specific lesions
 - = no lesions

Table 5.1. Source of isolates of M. paratuberculosis from red deer used for the cultural investigation

Source	No. from clinical cases	No. from sub-clinical cases
Farm A	2	38
Farm B	5	5
Other farms	0	4

Table 5.2. Growth rates of isolates of M. paratuberculosis made from mesenteric lymph nodes of naturally infected red deer during primary isolation on artificial medium

Source of isolate	No. of isolates examined	No. with growth visible after incubation for	
		4 weeks	>4-6 weeks
Clinical cases	7	3	4
Sub-clinical cases	47	8	39

Table 5.3. Recovery of isolate M928 of "M. paratuberculosis" from tissues of laboratory animals experimentally infected with the organism

Animal spp & No.	Median No. of colonies recovered on a pair of slopes inoculated with 10^{-1} dilution of tissue from					
	Site of injection/ draining lymph node	Intestines	Mesenteric lymph nodes	Spleen	Liver	Lungs
Rabbit	1	-/-	-	-	-	-
	2	-/-	-	-	-	-
G.pig	1	+++ / +++	-	-	+	-
	2	+++ / +++	-	-	+	-
	3	++ / ++	-	-	-	-
D.fowl	1	- / NE	+	NE	+	-
	2	- / NE	-	NE	+	+

+++ = organisms recovered in large numbers (>50 colonies)

++ = recovered in moderate numbers (10-50 colonies)

+ = recovered in small numbers (< 10 colonies)

- = not recovered

NE = not examined (organ not available)

FIGURES

Figure 3.1. Comparison of vaccinated and non-vaccinated red deer with severe and mild histopathological lesions of paratuberculosis in the mesenteric lymph nodes.

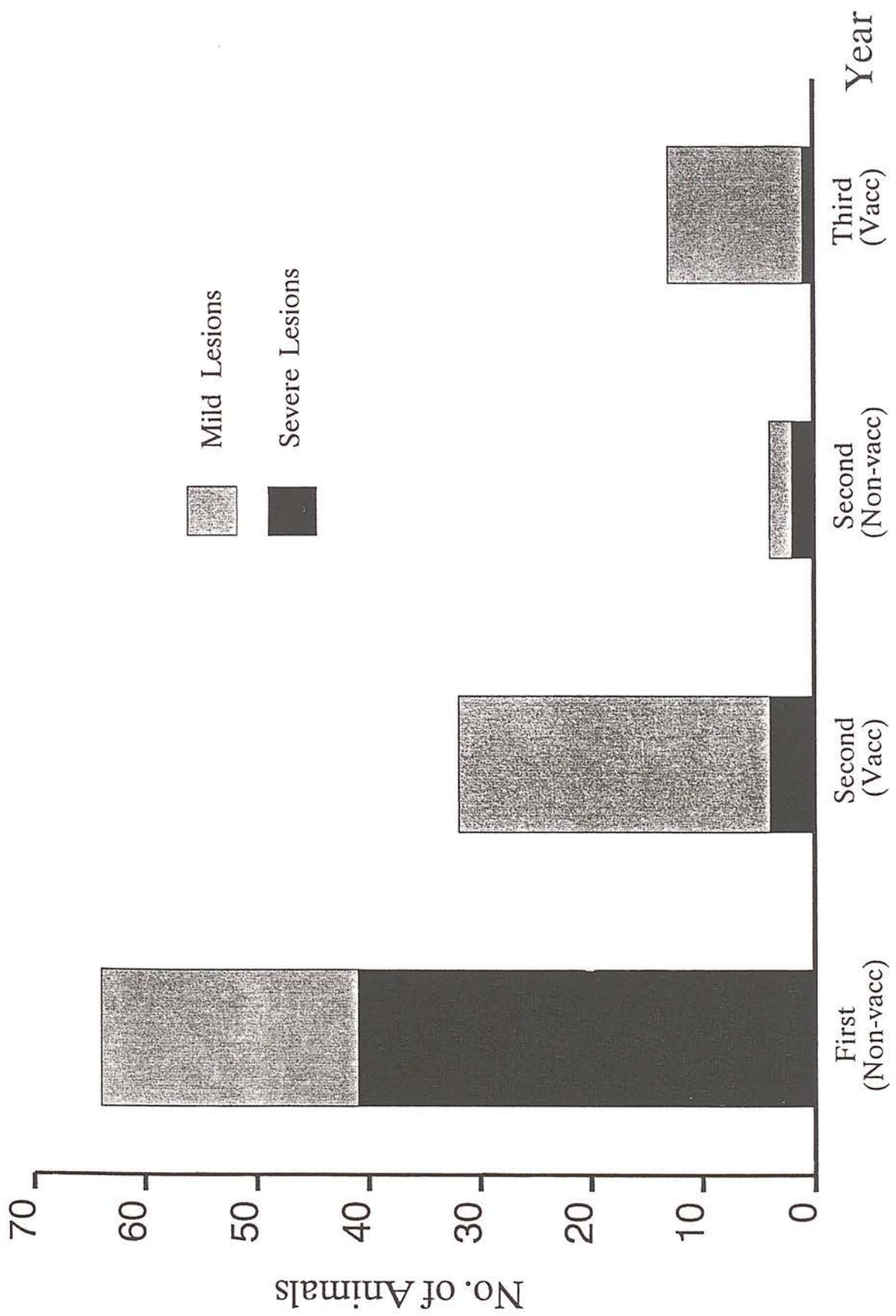


Figure 3.2. An adult red deer hind clinically affected with paratuberculosis. A natural infection. Note the poor bodily condition and rough hair coat.

Figure 3.3. A section of the small intestine and contiguous mesentery from the hind with paratuberculosis in Figure 3.2. Note oedema and thickening of the intestine and mesentery and the nodules (arrowed) along afferent lymphatic channels.



Figure 3.4. Irregular thickening and oedema of the mucosa of the section of the small intestine shown in Figure 3.3.

Figure 3.5. A section of the small intestine from a severely affected paratuberculous red deer with a natural infection. Note the irregularly thickened and haemorrhagic mucosa.

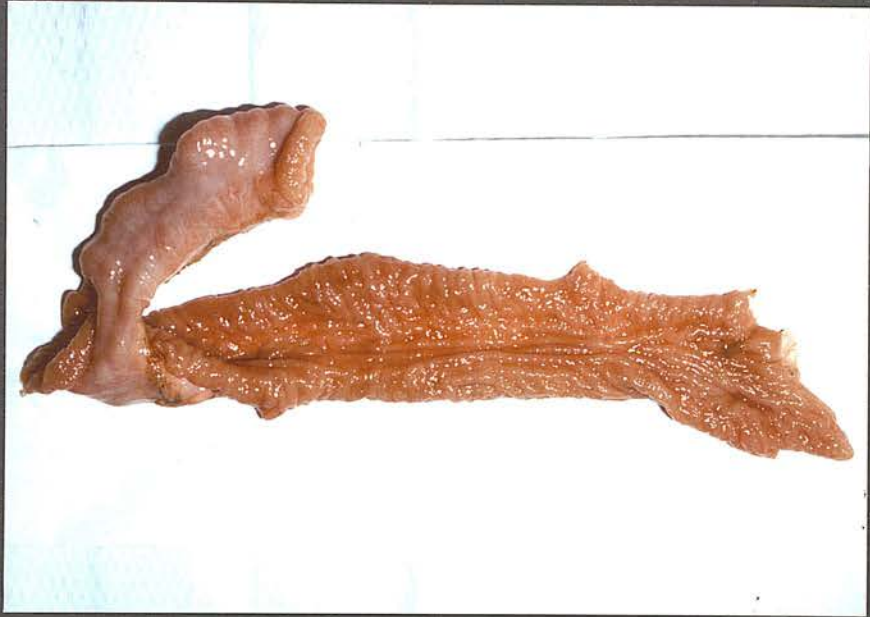


Figure 3.6. Granulomatous inflammation of the small intestine of the paratuberculous red deer in Figure 3.2 (H & E; x4).

Figure 3.7. Part of a villous tip from the section of the small intestine in Figure 3.6, showing accumulation of epithelioid cells (H & E; x40).

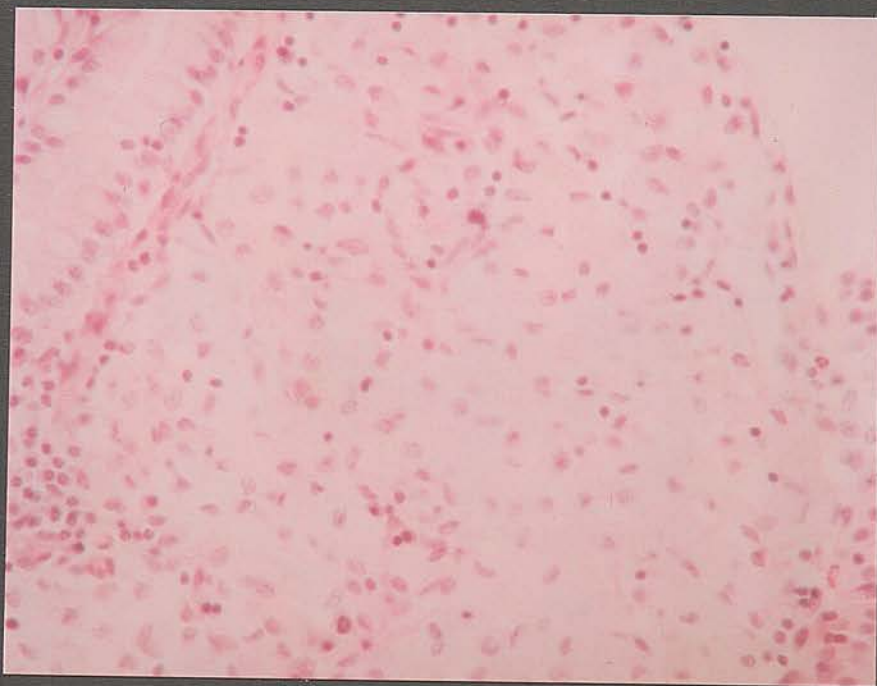
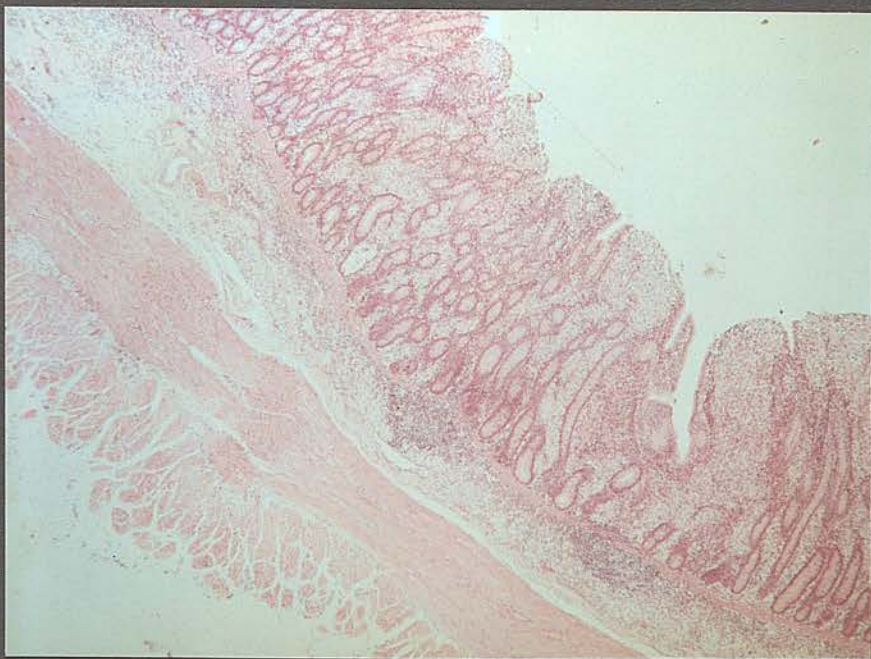


Figure 3.8. Diffuse granulomatous inflammation of the mucosa and submucosa of the small intestine of a severely affected paratuberculous red deer with a natural infection. Note focal necrosis (n) in the submucosa and extensive thickening of the mucosa and submucosa (H & E; x 10).

Figure 3.9. Clumps of AFB in the mucosa and submucosa of the small intestine. A serial section of Figure 3.6 (ZN; x4).

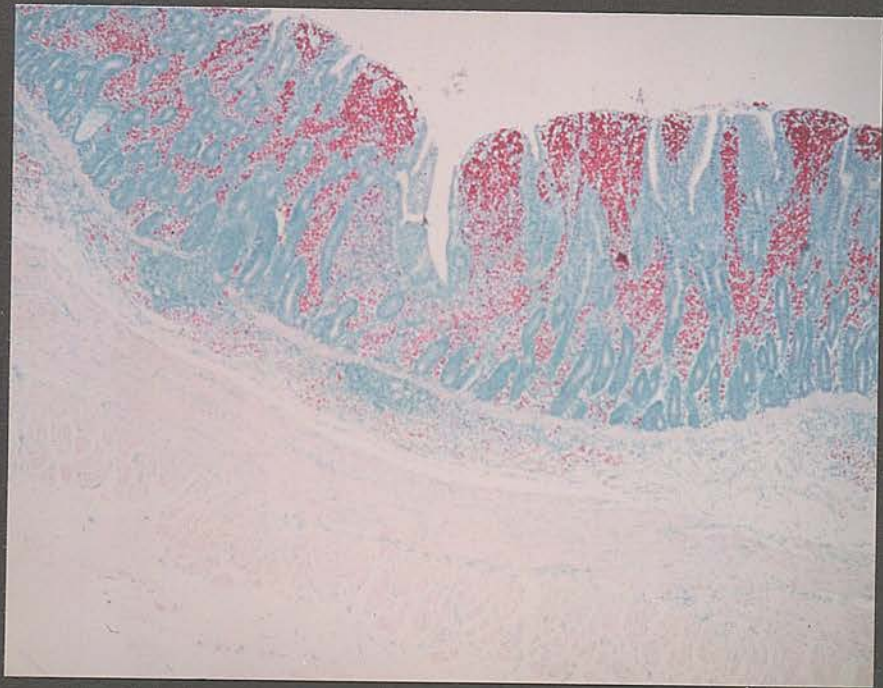
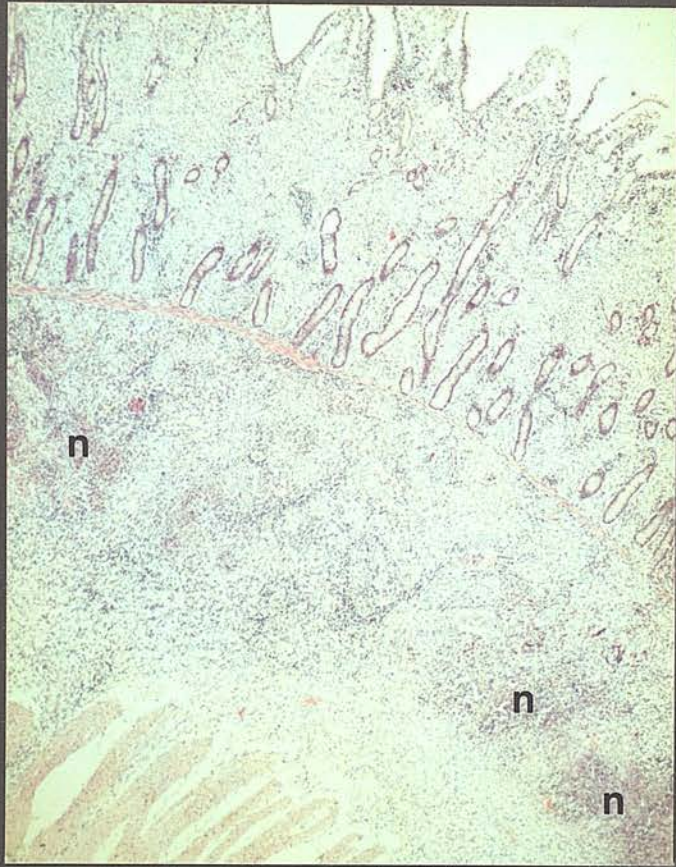


Figure 3.10. Haemorrhage and infiltration of lymphocytes and eosinophils in the mucosa of the small intestine of a paratuberculous red deer with a natural infection (H & E; x40).

Figure 3.11. Foci of epithelioid cell accumulation in the subcapsular (s) and paracortical (p) zones of a mesenteric lymph node from the hind with paratuberculosis in Figure 3.2 (H & E; x4).

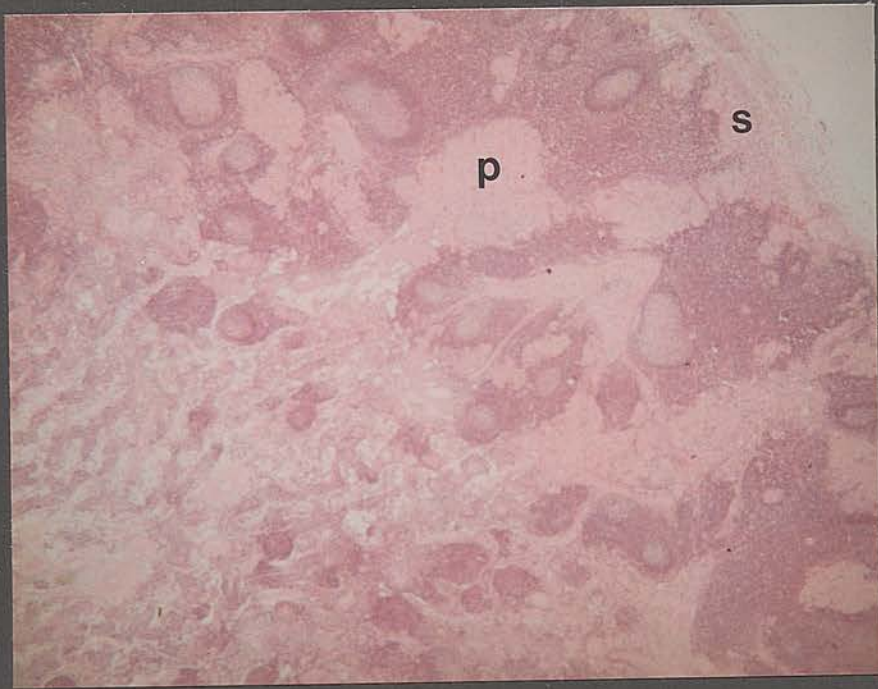
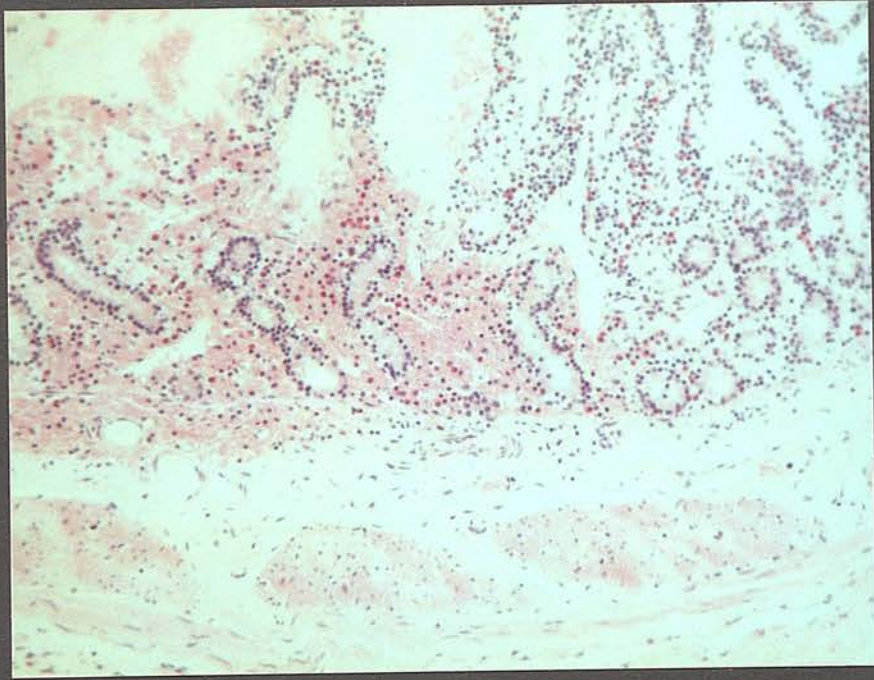


Figure 3.12. Granulomatous inflammation of a mesenteric lymph node from a red deer severely affected with paratuberculosis. Note the large focus of necrosis (N) (H & E; x10).

Figure 3.13. Clumps of AFB in a mesenteric lymph node from a paratuberculous red deer. A serial section of Figure 3.11. Note the absence of clumps in the medullary region (ZN; x4).

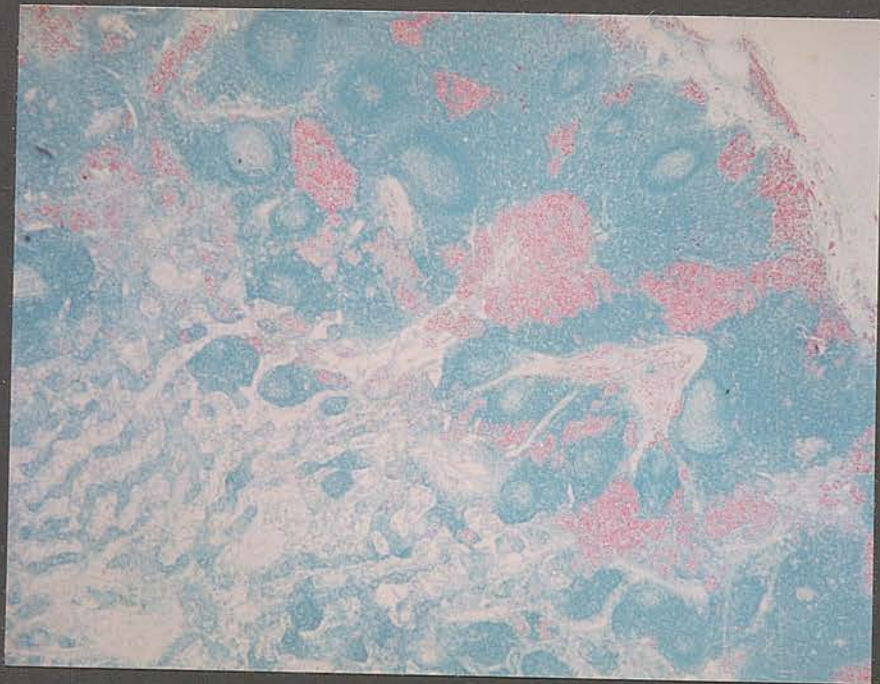
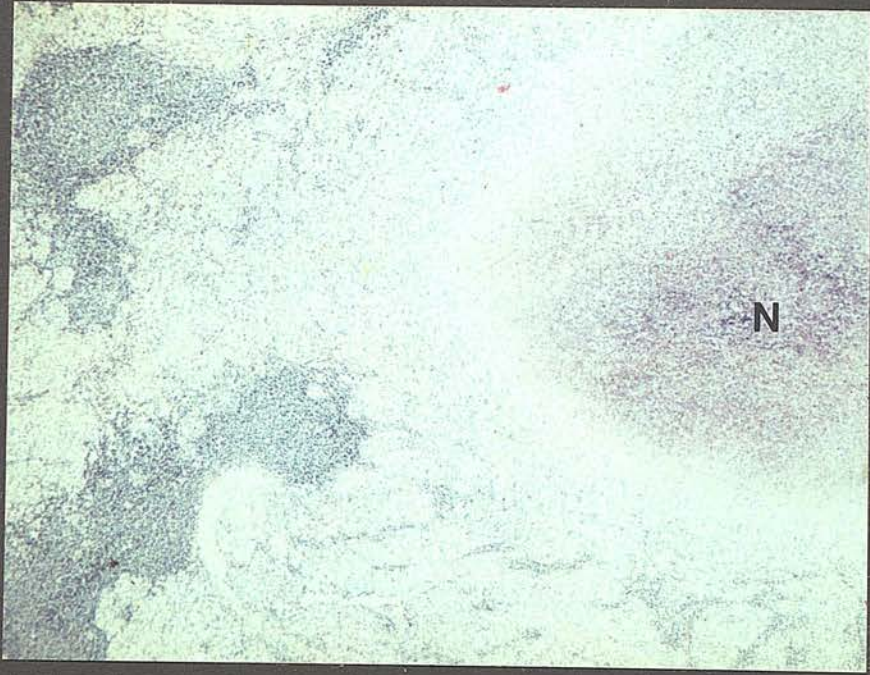


Figure 3.14. Non-specific degenerative changes in a mesenteric lymph node from a paratuberculous red deer. Note the accumulation of homogeneous eosinophilic deposits (D) in germinal centres of lymphatic nodules (H & E; x16).

Figure 3.15. A microgranuloma containing lymphoid cells and a few epithelioid cells and macrophages in the liver of the red deer in Figure 3.2 (H & E; x63).

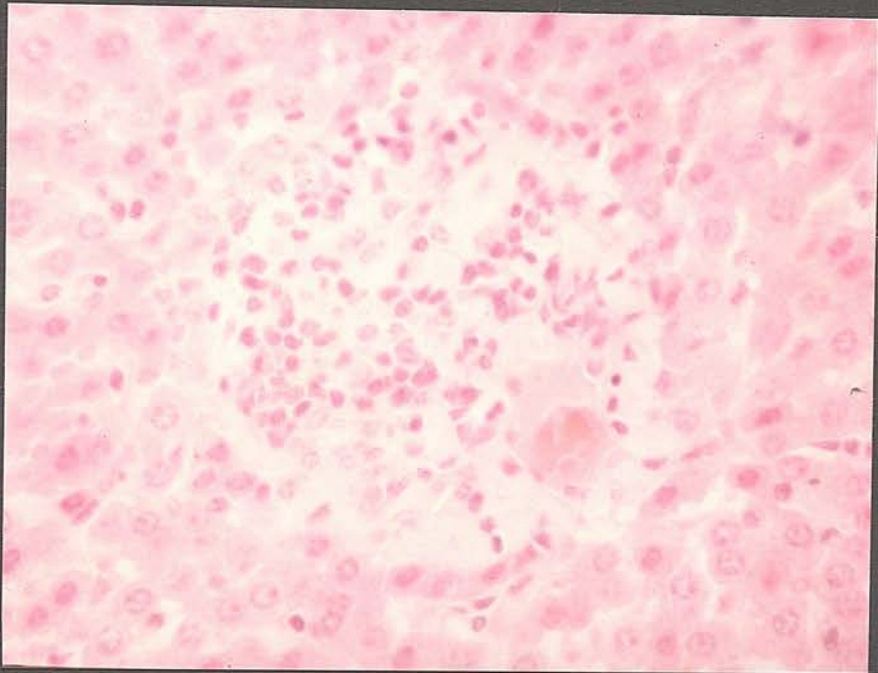


Figure 3.16. A clinically ill adult red deer hind affected with avian tuberculosis. A natural infection. Note the poor bodily condition, rough hair coat and loss of hair.

Figure 3.17. Markedly thickened intestinal wall and mesentery of the hind in Figure 3.16. Note the numerous prominently thickened, tortuous, knotted afferent lymphatic channels (arrowed).

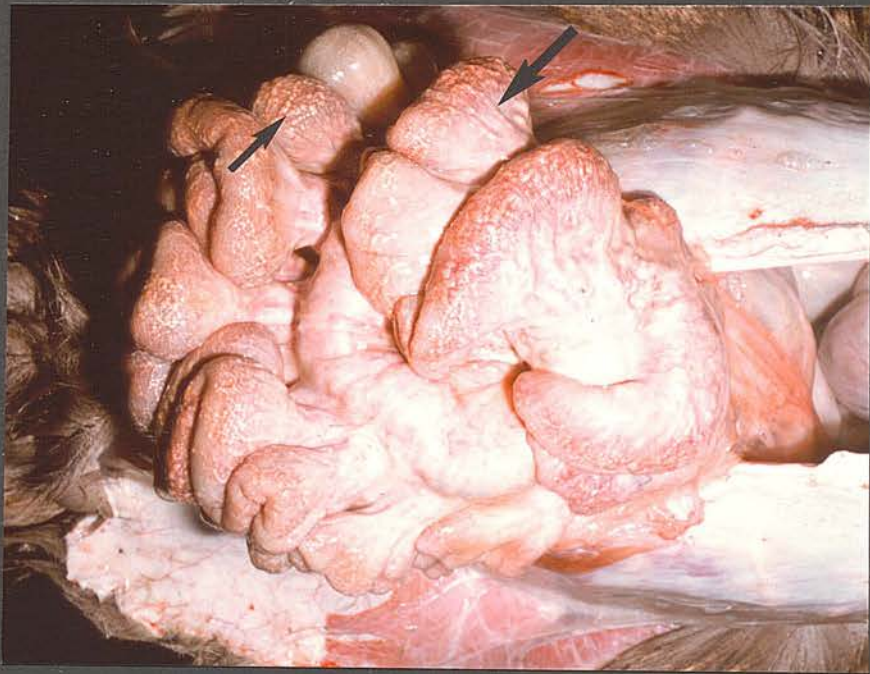


Figure 3.18. Sections of the small intestine from the red deer in Figure 3.16. Note irregular thickening and oedema of ileal mucosa (I), corrugation and haemorrhages of jejunal mucosa (J) and fairly normal duodenal mucosa (D).

Figure 3.19. Markedly enlarged and indurated mesenteric lymph nodes (N) from the deer in Figure 3.16.

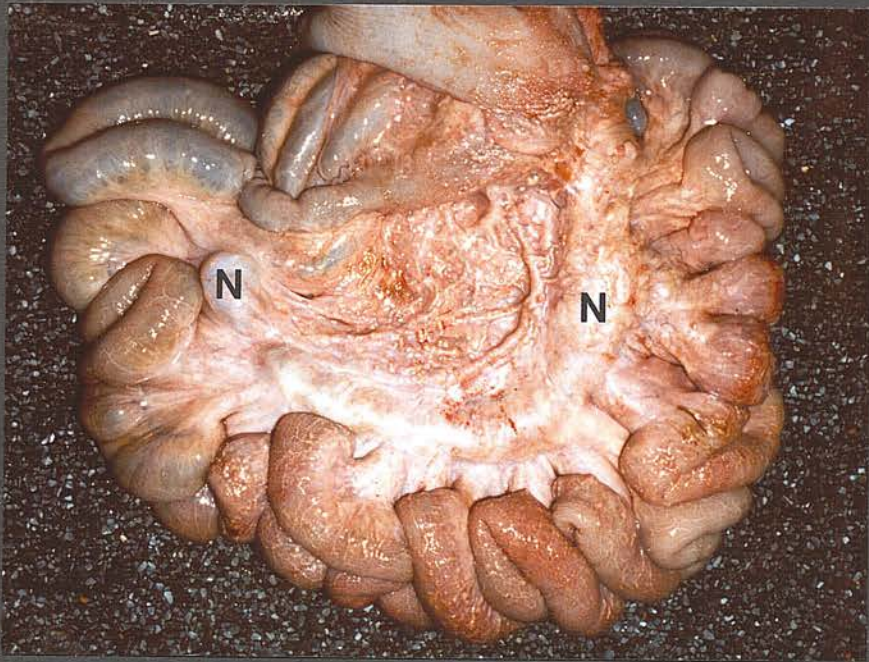
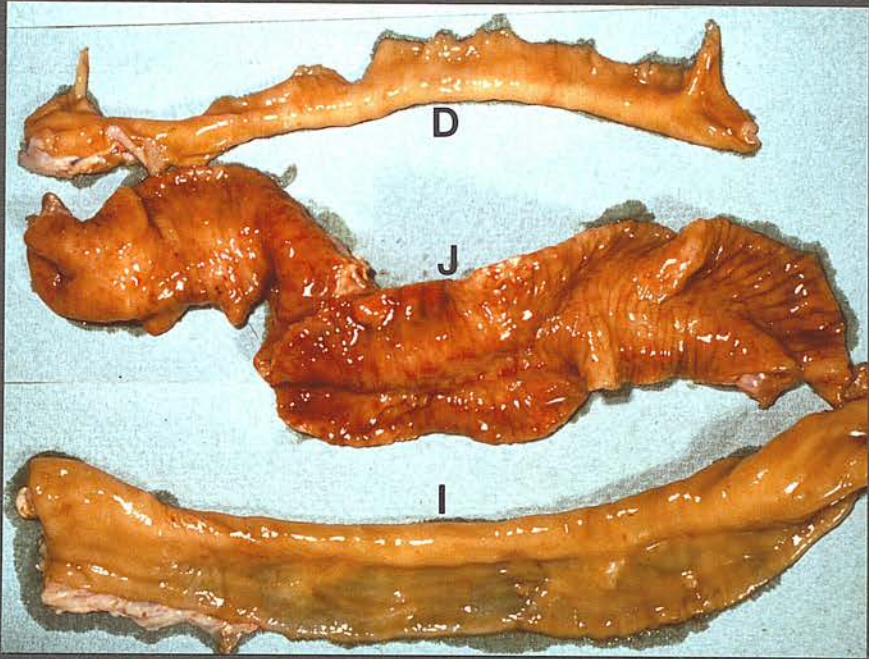


Figure 3.20. Accumulations of epithelioid cells in villous tips of the small intestine of the hind in Figure 3.16 (H & E; x40).

Figure 3.21. A lymphatic follicle in the submucosa of the small intestine of the deer in Figure 3.16 surrounded and infiltrated by epithelioid cells and macrophages (H & E; x40).

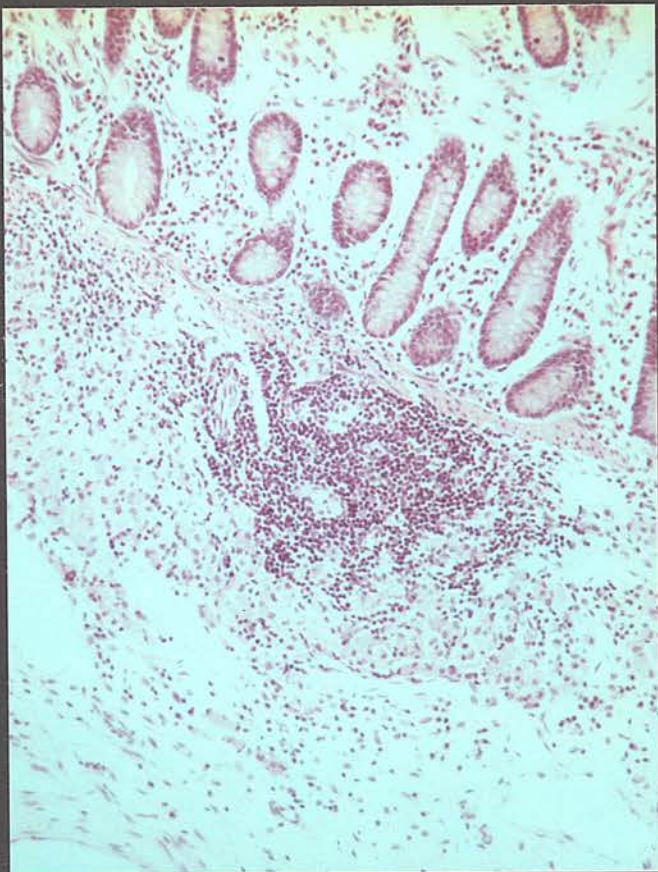
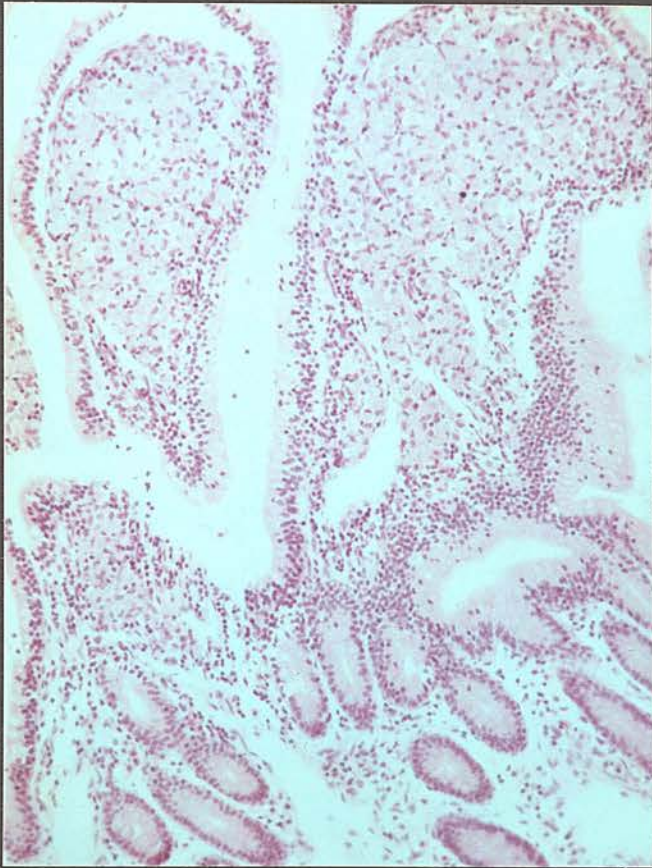


Figure 3.22. Clumps of AFB in the mucosa, submucosa and serosa of the small intestine from the hind in Figure 3.16. Note the concentration of the clumps in the villous tips (V), around the lymphatic follicle (F) and the focal granulomas (S) in the serosa (ZN; x10).

Figure 3.23. Granulomatous inflammation of the mesentery accompanied by vascular thickening in the red deer shown in Figure 3.16 (H & E; x16).

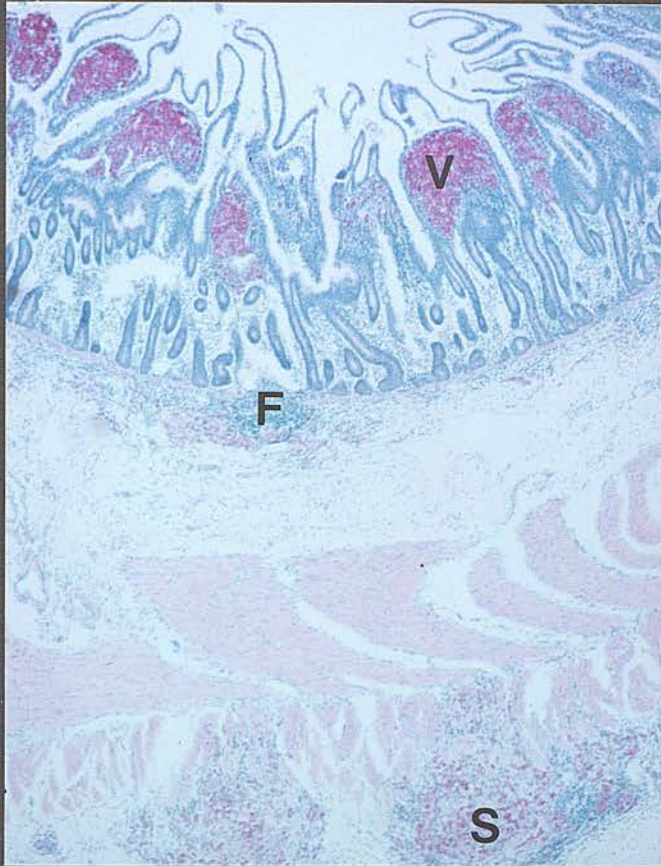


Figure 3.24. Focal aggregation of epithelioid cells and macrophages in loose lymphatic tissue of a tonsil from the red deer in Figure 3.16 (H & E; x 40).

Figure 3.25. Islets of epithelioid cells, macrophages and giant cells in a splenic corpuscle of the spleen from the red deer in Figure 3.16 (H & E; x 40).

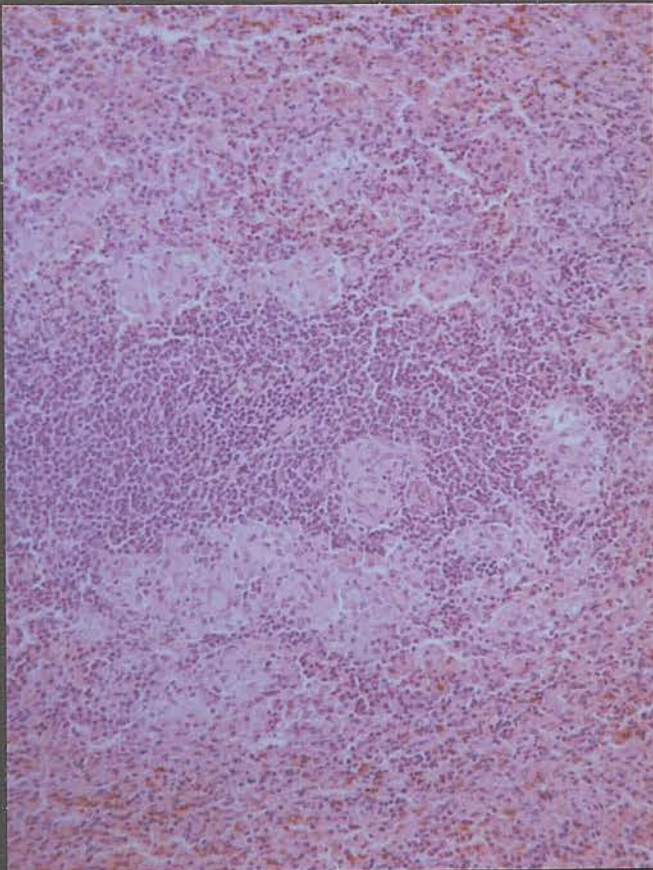
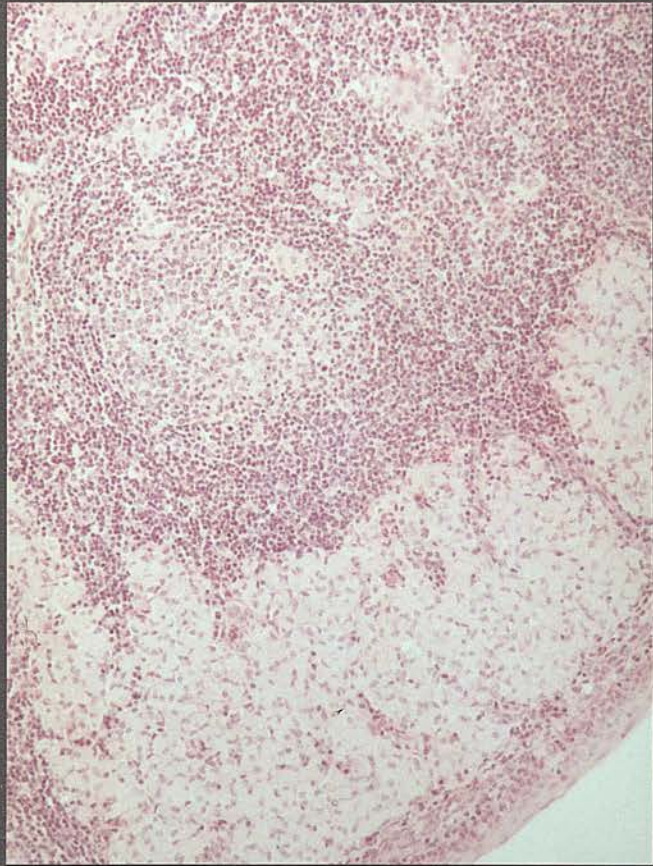


Figure 3.26. Glomerular tuft of a renal tubule infiltrated by epithelioid cells and macrophages, from a kidney of the the hind in Figure 3.16 (H & E; x40).

Figure 3.27. A section of a lung from the red deer in Figure 3.16. Note the thickened interalveolar walls due to infiltration and accumulation of epithelioid cells and macrophages (H & E; x40).

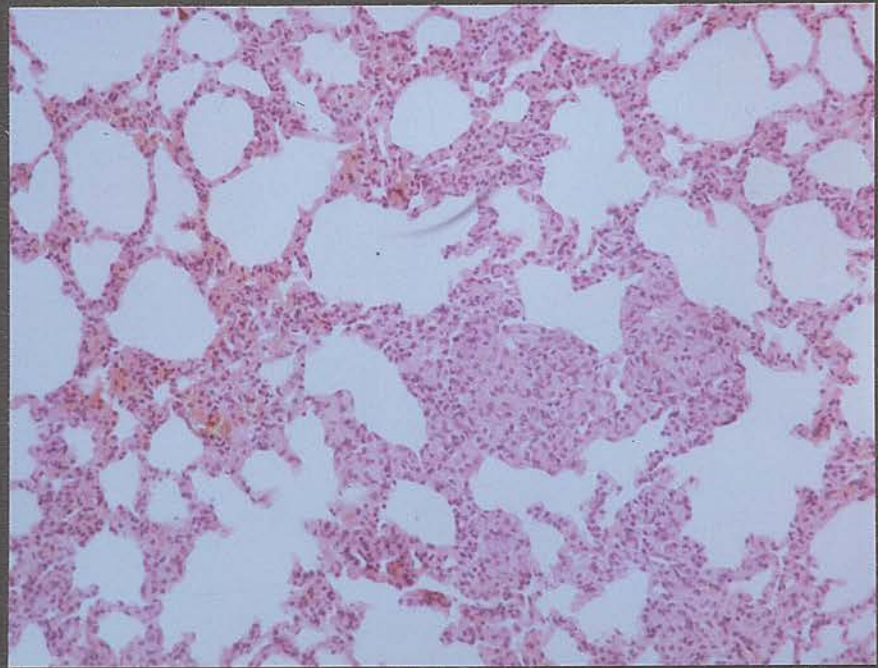
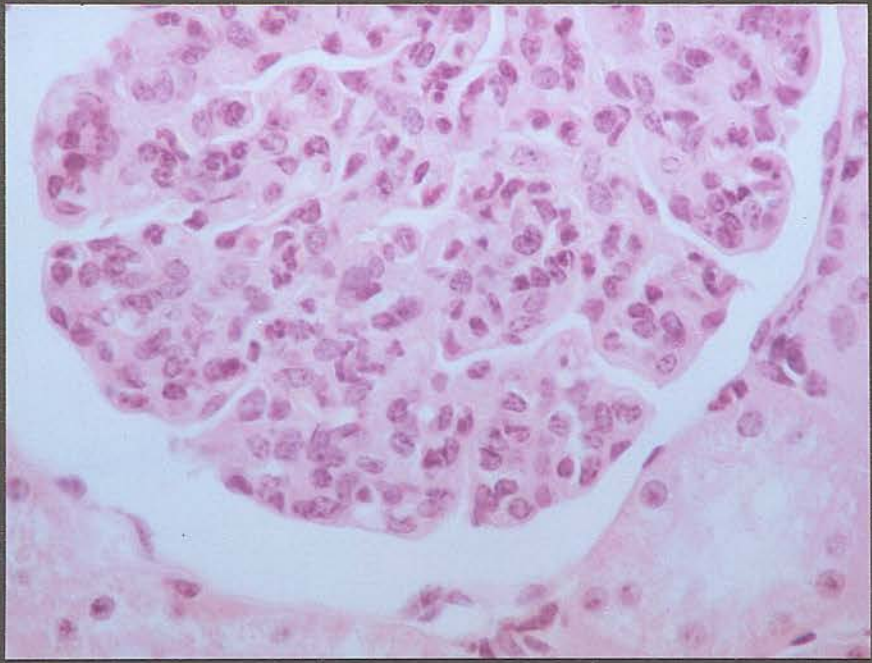


Figure 3.28. Miliary granulomas in the spleen (S) and liver (L) of a domestic fowl experimentally infected with M. avium isolated from the deer in Figure 3.16.

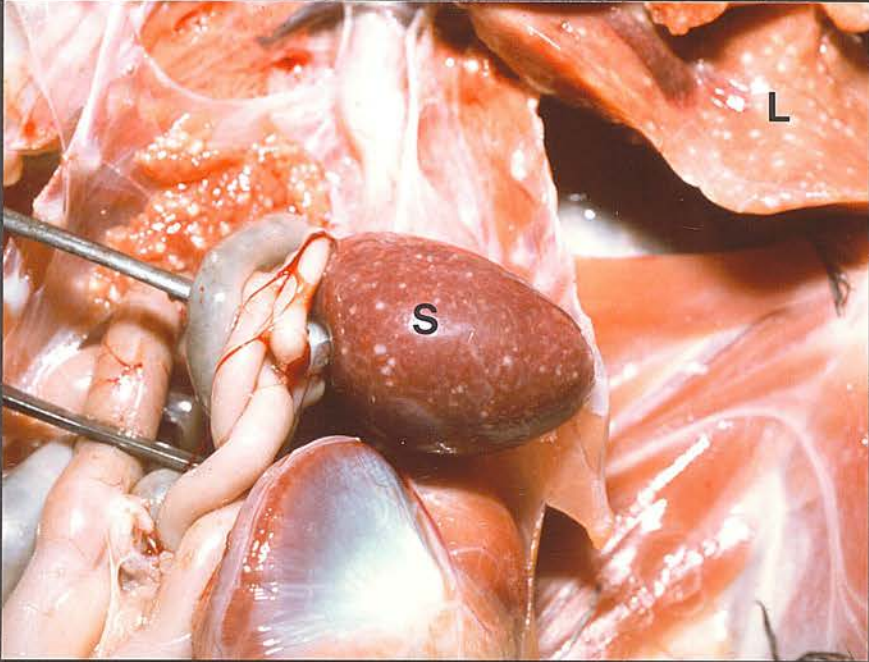


Figure 4.1. A clinically ill red deer calf (forefront) with experimentally induced paratuberculosis. Note the small size of the animal compared with the others of the same age in the group.

Figure 4.2. Clinically sick red deer calves affected with experimentally induced avian tuberculosis.



Figure 4.3. Serological response of red deer experimentally dosed with M. paratuberculosis determined by ELISA. Cut-off OD = 0.04 (Raw data in Appendix 3).

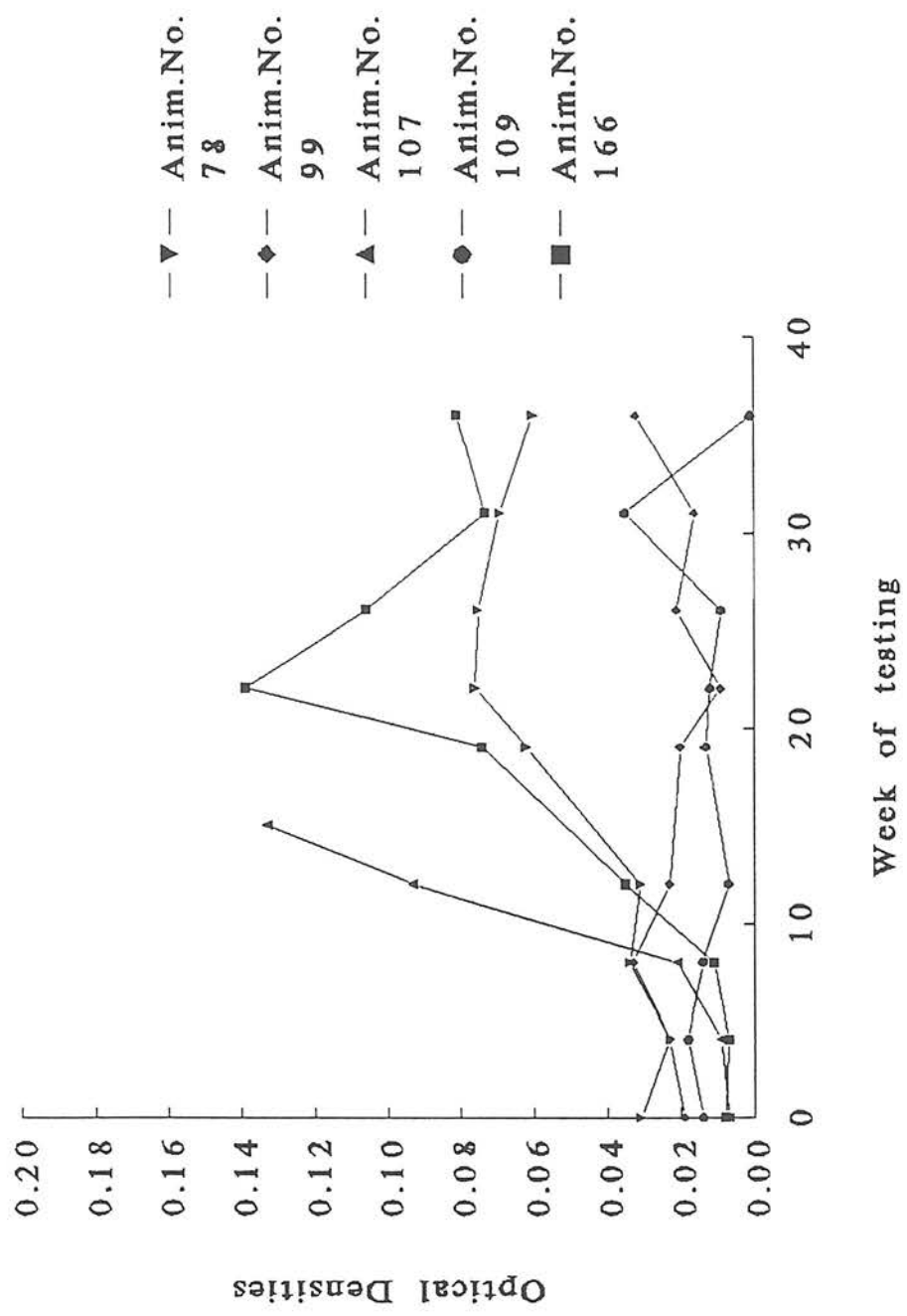


Figure 4.4. Severe granulomatous inflammation in the region of a Peyer's patch in the small intestine of a red deer calf with experimentally induced paratuberculosis. Note the marked thickening, extensive necrosis and focal mineralization (M) of the submucosa and ulceration (U) of the mucosa (H & E; x10).

Figure 4.5. A section of the small intestine and contiguous mesentery from a red deer calf experimentally infected with M. paratuberculosis. Note the diffuse accumulation of granulomatous cells in the mucosa and peri- (p) and endo- (e) lymphangitis and vascular thickening (V) in the mesentery (H & E; x10).

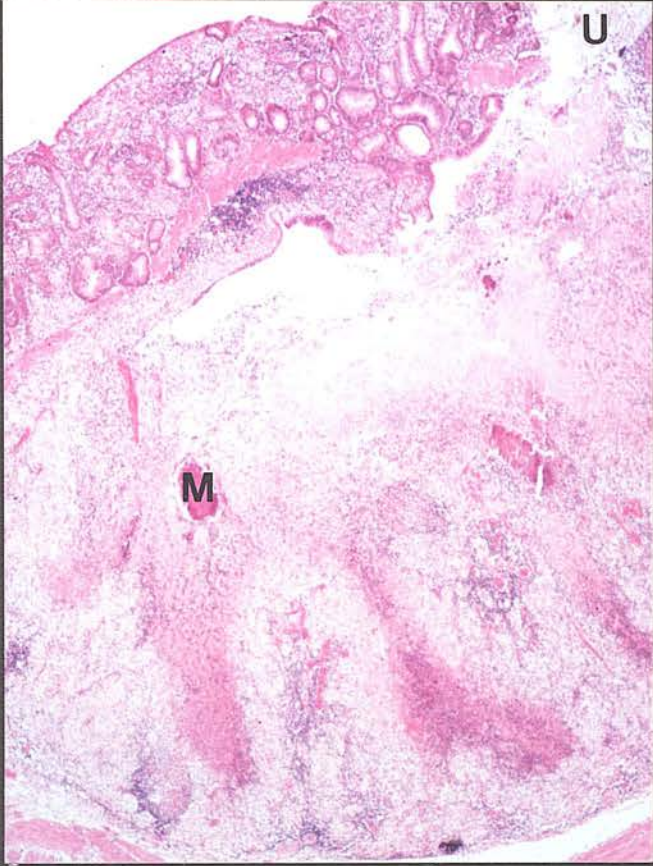


Figure 4.6. A granulomatous lesion in the submucosa of the ileocaecal valve of a red deer calf experimentally infected with M. paratuberculosis (H & E; x 40).

Figure 4.7. Granulomatous inflammation of a mesenteric lymph node from a red deer calf with experimentally induced paratuberculosis. Note the focal necrosis and mineralization (NM) (H & E; x16).

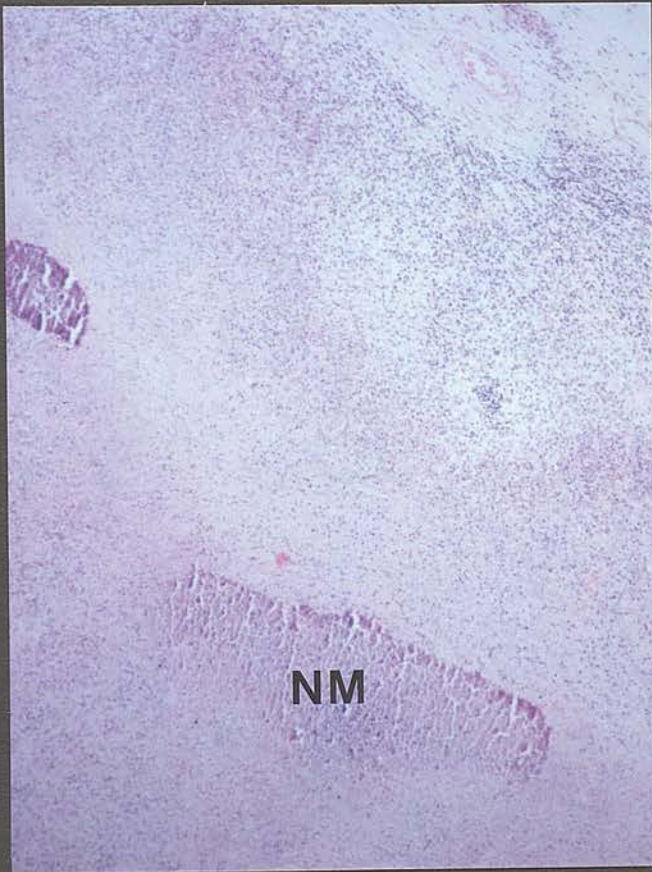
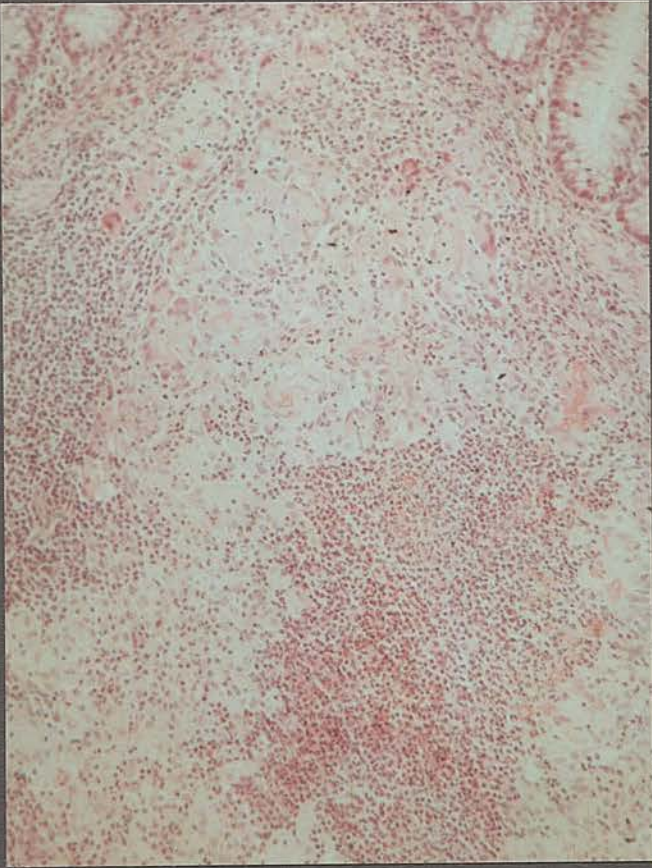


Figure 4.8. Irregular thickening, haemorrhage and ulceration of the mucosa of the small intestine of a red deer calf experimentally infected with M. avium.

Figure 4.9. Granulomatous inflammation of the small intestine from a calf experimentally infected with M. avium. Note the erosion, ulceration (U) and focal granuloma (arrowed) of the mucosa and the extensively thickened submucosa containing markedly enlarged lymphatic follicles (H & E; x4).

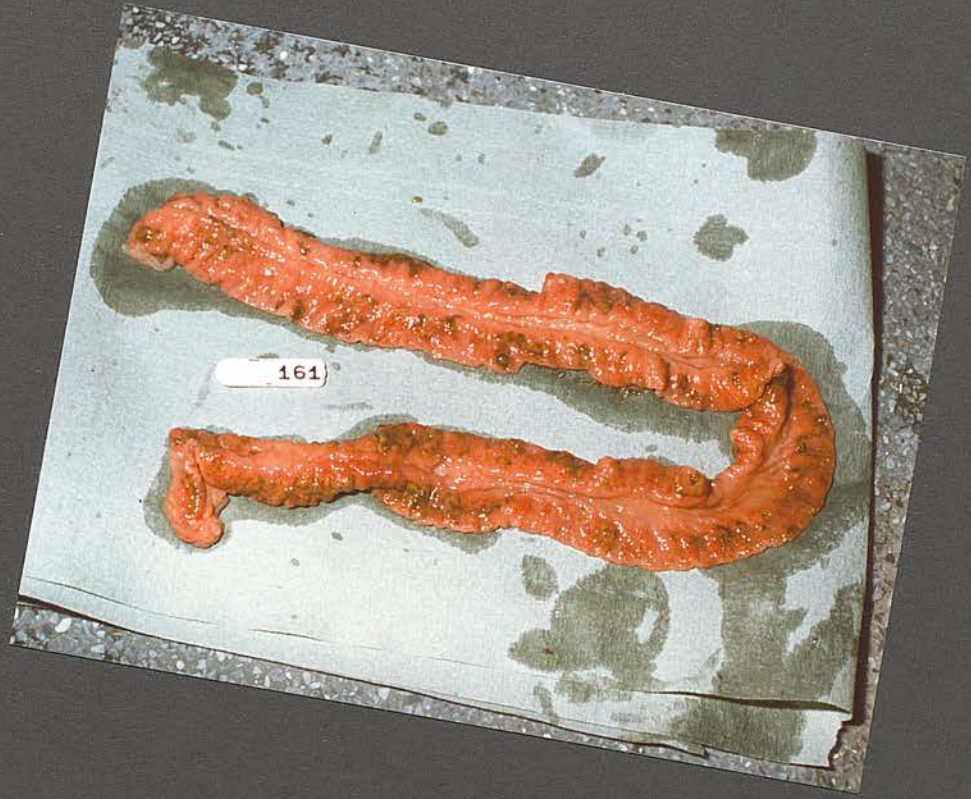


Figure 4.10. A microgranuloma in the mucosa of the small intestine in Figure 4.9 (H & E; x40).

Figure 4.11. Thickened serosa of the small intestine in Figure 4.9. Note the focal granulomas and asymmetrical thickening of the lymphatic channel (L) (H & E; x 40).

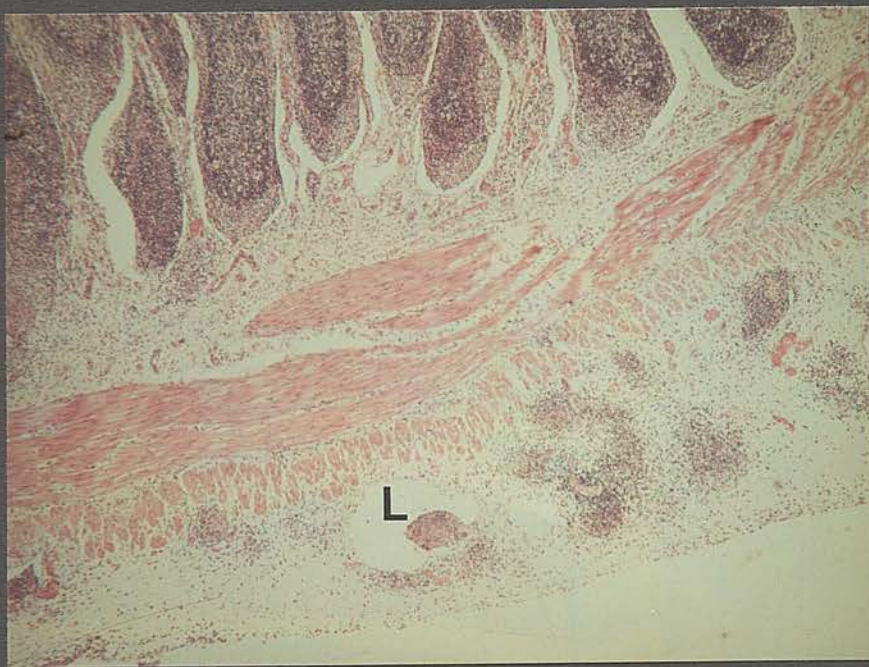
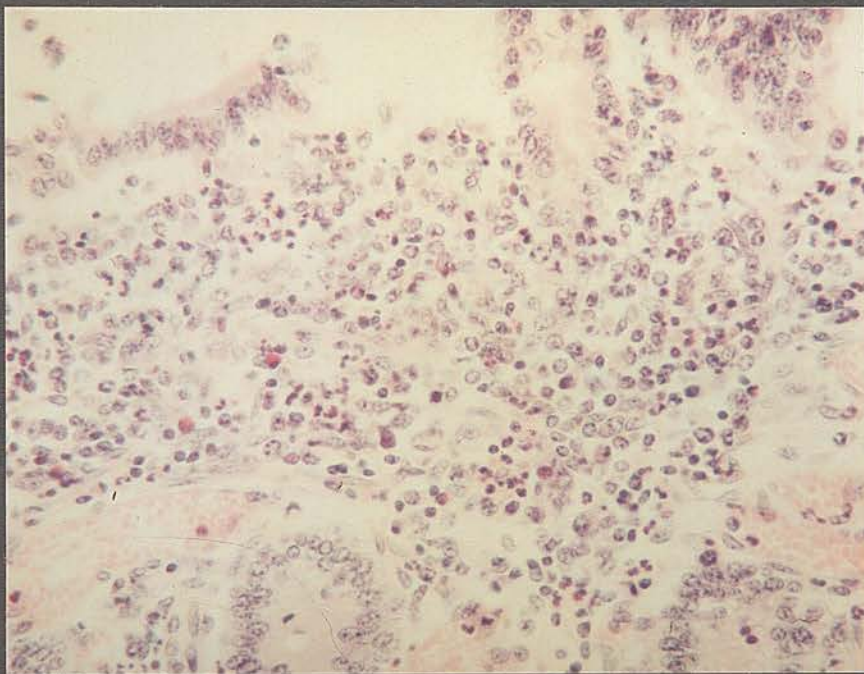


Figure 4.12. Partial obliteration of an afferent lymphatic channel in the serosa of the small intestine in Figure 4.9 (H & E; x40).

Figure 4.13. Discrete nodules (arrowed) in the wall of the small intestine of a lamb experimentally infected with M. paratuberculosis.

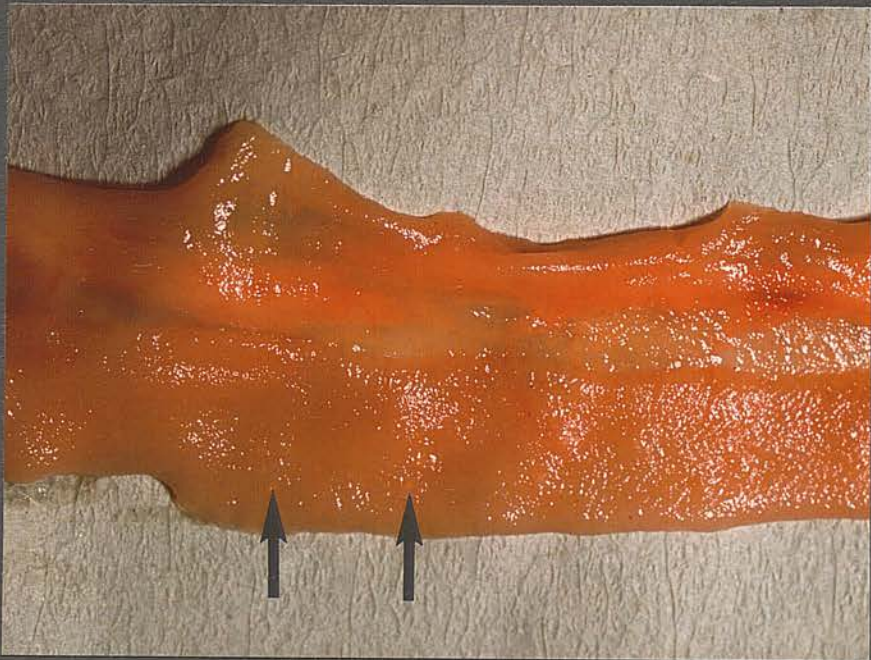
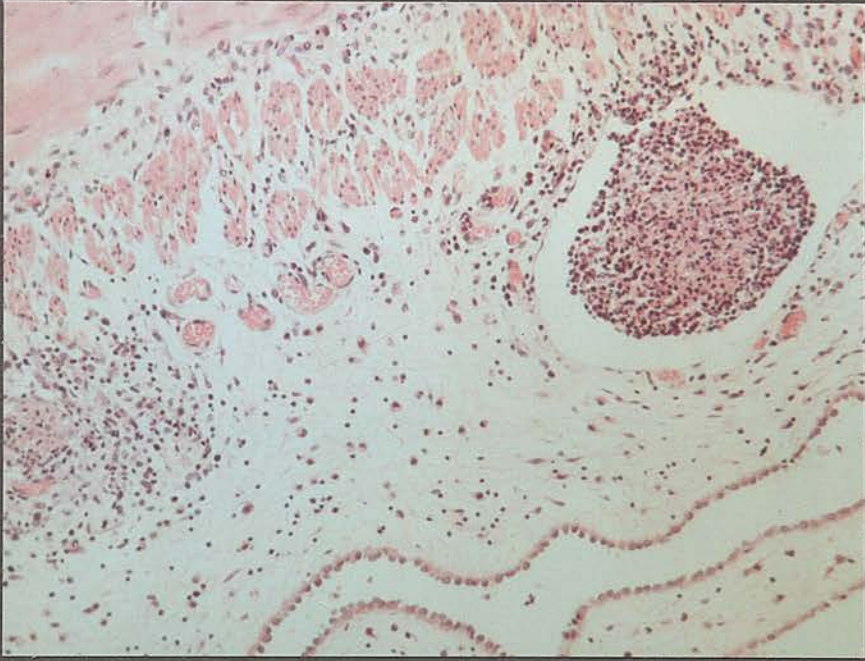


Figure 4.14. Granulomatous inflammation of the submucosa of the terminal ileum of a lamb experimentally infected with M. paratuberculosis. Note marked thickening of the submucosa accompanied by necrosis (H & E; x10).

Figure 4.15. A tuberculoid granuloma in the submucosa of the ileocaecal valve of a lamb experimentally infected with M. paratuberculosis. Note walling-off of the lesion (H & E; x40).

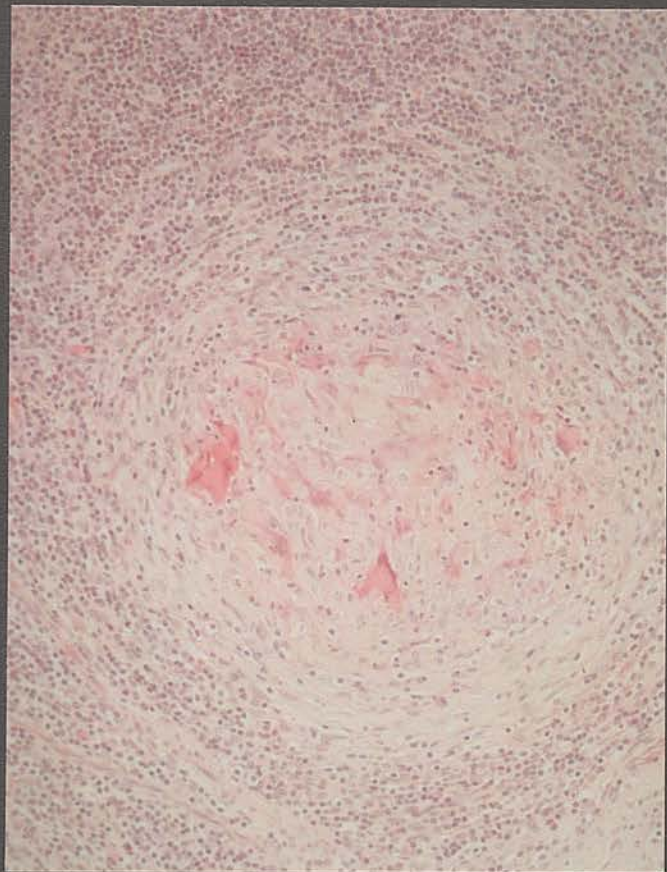


Figure 4.16. A necrotic granuloma in the submucosa of the ileocaecal valve of a lamb experimentally infected with M. paratuberculosis (H & E; x 40).

Figure 4.17. Tuberculoid (T) and extensive (E) granulomas in a mesenteric lymph node from a lamb experimentally infected with M. paratuberculosis. Note the extensive necrosis of E (H & E; x16).

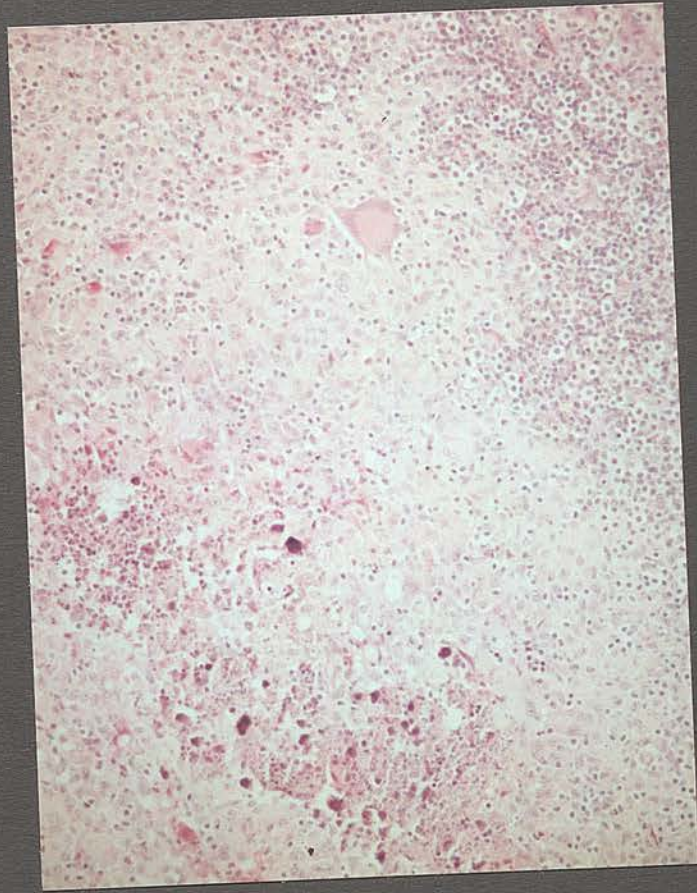


Figure 6.1. Polypeptides of isolates of M. paratuberculosis from deer (lanes A and D), a cow (lane E) and a goat (lane F), isolate M928 (lane B), PPA-3 (lane G) and an isolate of M. avium (lane C) separated by SDS-PAGE and stained with Coomassie blue. Lane M, molecular weight markers (kDa). Note the doublet (arrowed) in isolate M928 and the polypeptide (arrowed) of approximately 38-40 kDa in the PPA-3 and M. avium isolate.

Figure 6.2. Polypeptides of PPA-3 (lane A), an isolate of M. ptbc from deer (lane B) and isolate M928 (lane C) separated by SDS-PAGE and stained with Coomassie blue. Lane M, molecular weight markers (kDa). Note the doublet (arrowed) in isolate M928 and the polypeptide (arrowed) of approximately 38-40 kDa in the PPA-3.

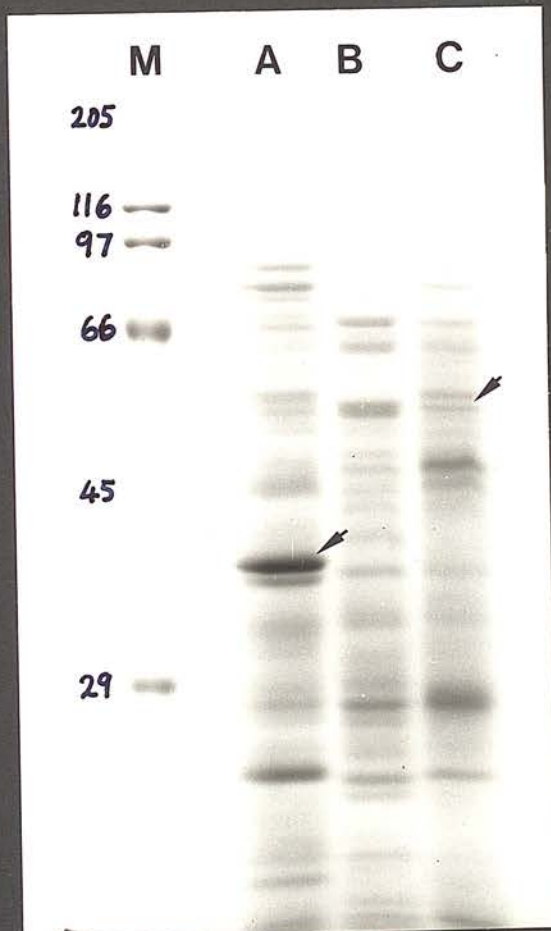
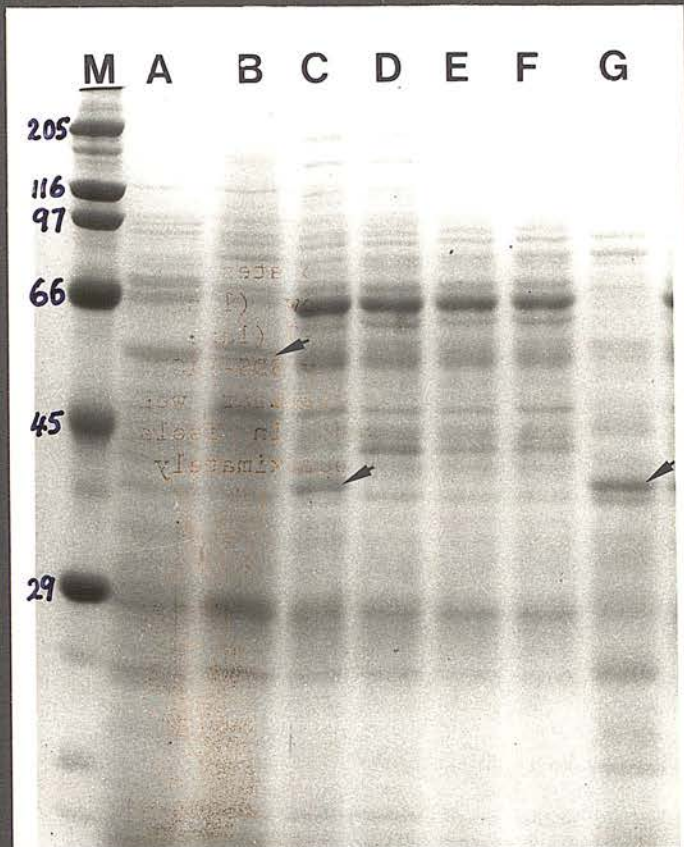


Figure 6.3. Polypeptides of isolates of M. paratuberculosis from deer (lanes A-F), a cow (lane G) and a goat (lane H), isolate M928 (lane I), PPA-3 (lane X) and isolates of M. avium (lanes 1-9) separated by SDS-PAGE and stained with Coomassie blue. Lane W, molecular weight markers (kDa). Note the polypeptide (arrowed) of approximately 38-40 kDa in the M. avium isolates and the PPA-3.

Figure 6.4. A Western blot showing SDS-PAGE separated polypeptides of isolates of M. paratuberculosis from deer (lanes A-C) and of isolate M928 (lane D) recognized by paratuberculosis-positive deer serum. The molecular weights in kDa are shown on the left of lane A. Note the displacement of the polypeptide (arrowed) and absence of some of the polypeptides in isolate M928 compared with the M. paratuberculosis isolates.

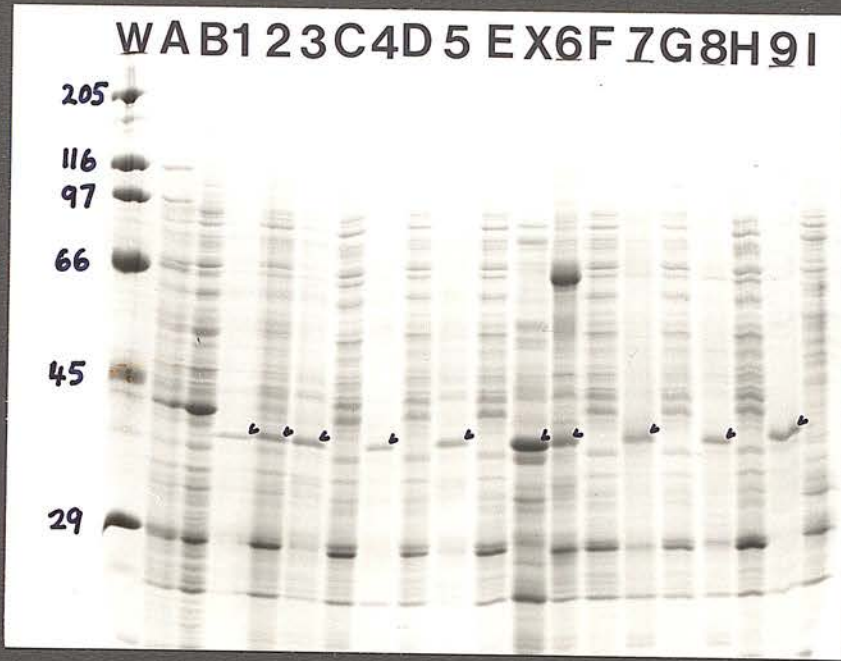


Figure 6.5. A Western blot showing SDS-PAGE separated polypeptides of isolates of M. paratuberculosis from deer (lane B), a cow (lane C) and a goat (lane D), isolate M928 (lane A), PPA-3 (lane E) and an isolate of M. avium (lane F) recognized by paratuberculosis-positive deer serum. The molecular weights in kDa are shown on the left of lane A. Note the absence of some of the polypeptides in isolate M928 and the presence of two polypeptides (arrowed) in the PPA-3 not evident in the others. Note also the presence of the polypeptide labelled a in the PPA-3 and in the M. avium isolate (faint in the latter).

Figure 6.6. A Western blot showing SDS-PAGE separated polypeptides of isolates of M. paratuberculosis from deer (lanes A-C) and of isolate M928 (lane D) recognized by paratuberculosis-positive sheep serum. The molecular weights in kDa are shown on the left of lane A. Note the presence of very pronounced polypeptides in the 45 kDa to 66 kDa region. Note also the displacement of the polypeptide (arrowed) and presence of faint polypeptide bands in the 29-45 kDa region in isolate M928.

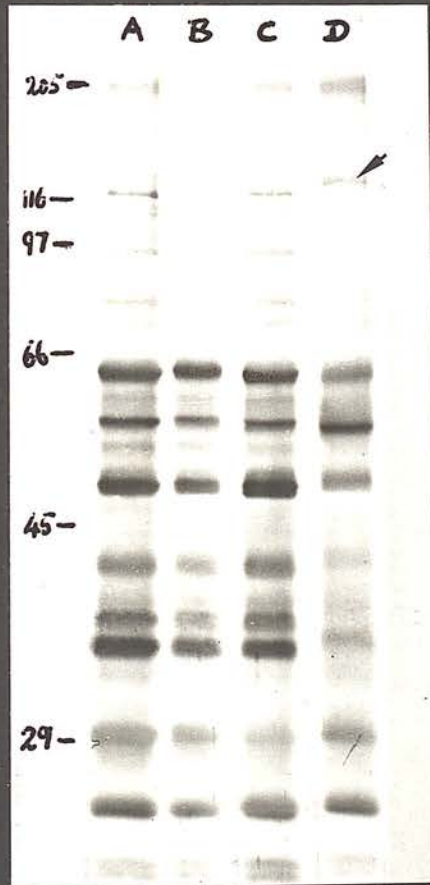
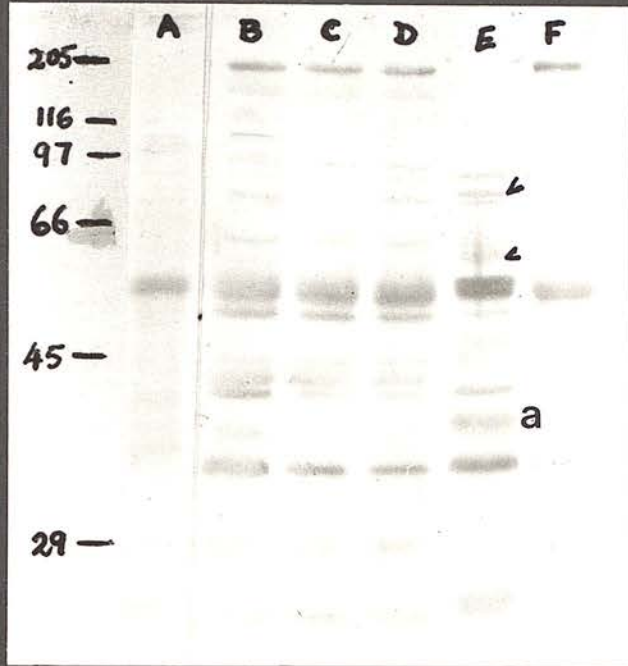


Figure 6.7. A Western blot showing SDS-PAGE separated polypeptides of M. paratuberculosis from deer (lane B), a cow (lane C) and a goat (lane D), isolate M928 (lane A), PPA-3 (lane E) and an isolate of M. avium (lane F) recognized by avian tuberculosis-positive deer serum. The molecular weights in kDa are shown on the left of lane A. Note the presence of the two polypeptides (arrowed) in the PPA-3 and the polypeptide (a) of approximately 38-40 kDa in the PPA-3 and the M. avium isolate (faint in the latter).

Figure 6.8. A Western blot showing SDS-PAGE separated polypeptides of an isolate of M. paratuberculosis from deer (lane A) and of isolates of M. avium (lanes B-E) recognized by avian tuberculosis-positive deer serum. The molecular weights in kDa are shown on the left of lane A. Note the presence of the polypeptide (arrowed) of approximately 38-40 kDa in the isolates of M. avium but not in the M. paratuberculosis isolate.

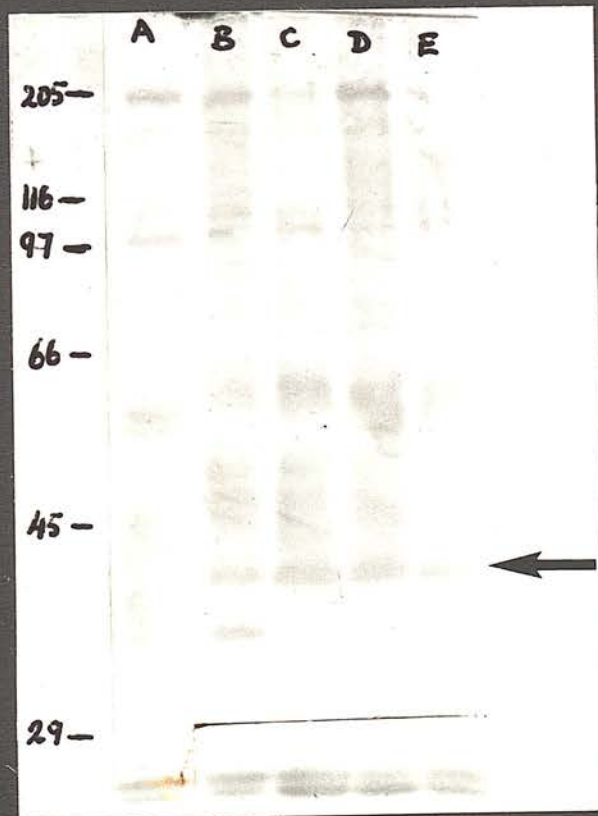
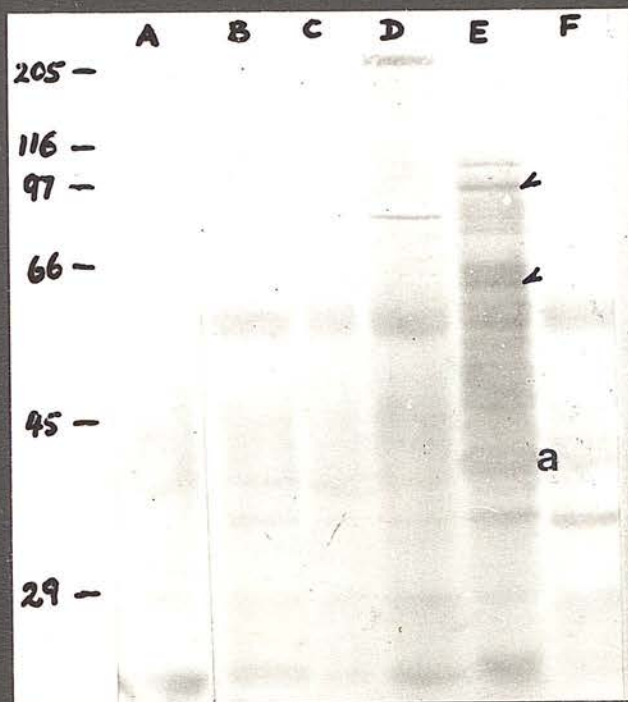


Figure 6.9. Detection of isolates of M. paratuberculosis among 18 isolates of mycobacteria by PCR-amplification of the 279 bp DNA fragment (arrowed) of the insertion element IS900 specific for M. paratuberculosis. Lane M, molecular weight markers (kb); lane A, positive standard plasmid DNA (pPN14); lanes B-J, isolates of M. avium; lanes 1-8, isolates of M. paratuberculosis from deer (1-6), a cow (7) and a goat (8); and lane 9, isolate M928.

Figure 6.10. A pattern-type obtained after hybridization of radiolabelled PCR279 DNA probe to Southern transferred BamHI DNA digests of eight isolates of M. paratuberculosis. Lanes A-F, isolates from deer; lane G, from a cow; and lane H, from a goat.



Figure 6.11. A pattern-type obtained after hybridization of radiolabelled PCR279 DNA probe to Southern transferred PstI DNA digests of eight isolates of M. paratuberculosis. The isolates are from a goat (lane 1), a cow (lane 2) and deer (lanes 3-8).

Figure 6.12. A pattern-type obtained after hybridization of radiolabelled PCR279 DNA probe to Southern transferred EcoRI digests of eight isolates of M. paratuberculosis. Lanes A-F, isolates from deer; lane G, from a cow; and lane H, from a goat. Molecular weights in kb are shown on the left of lane A. Note the presence of a RFLP indicated by the absence in the bovine isolate (lane G) of the fragment arrowed in the deer isolate (lane A).

